Electronic Supplementary Material (ESI) for Physical Chemistry Chemical Physics.

Supporting Information : Hydrophobic Dye Solubilization via Hybrid Imogolite Nanotube probed by Second Harmonic Scattering

Ali Dhaini[a], Fadwa Alfadel Raad[b], Antoine Thill[b], Benedicte Prelot [a], Gaelle Martin-Gassin[a] , Pierre-Marie Gassin[a] *

a. ICGM, Univ Montpellier, ENSCM, CNRS, Montpellier, France.
b. LIONS, NIMBE, CEA, CNRS, Université Paris-Saclay, 91191 Gif sur Yvette, France.

1°) Experimental SHS polar plots of pure water and water with IMO-CH3

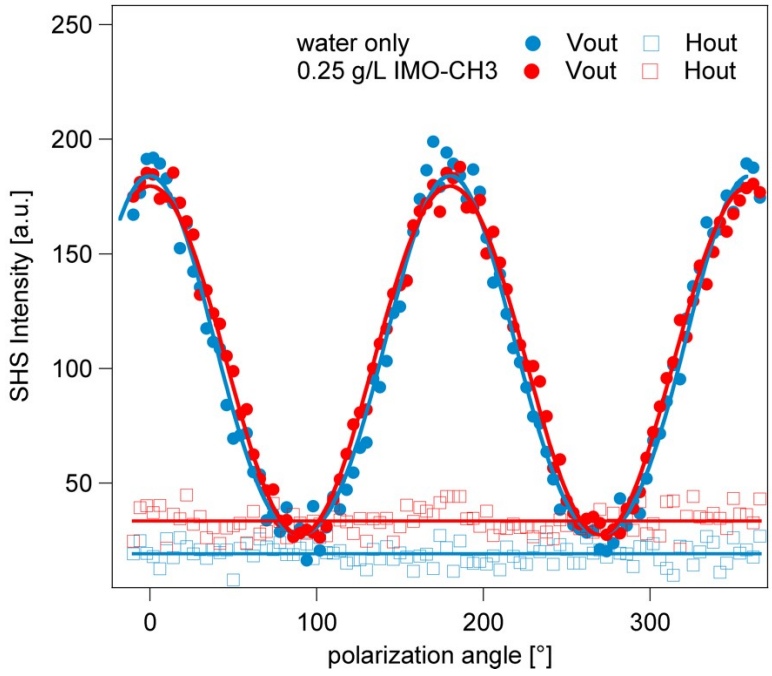

Figure S1 : polarization plot of pure water (blue point) and imogolite suspension at 0.25 g/L in water (red point). The lines are a fit according to equation (2) of the manuscript

The Figure S1 shows that the SHS polar plots are very close between pure water and imogolite suspension at 0.25 g/L. The main difference is a small increase of the Hout intensity.

This arises because of a water contribution coming from the organized and oriented water onto the external hydrophilic surface of the nanotube as explained in a this work[1]. At the concentration of 0.25 g/L the solution is absolutely not turbid and it can be seen on the UV vis absorbance spectrum presented below.

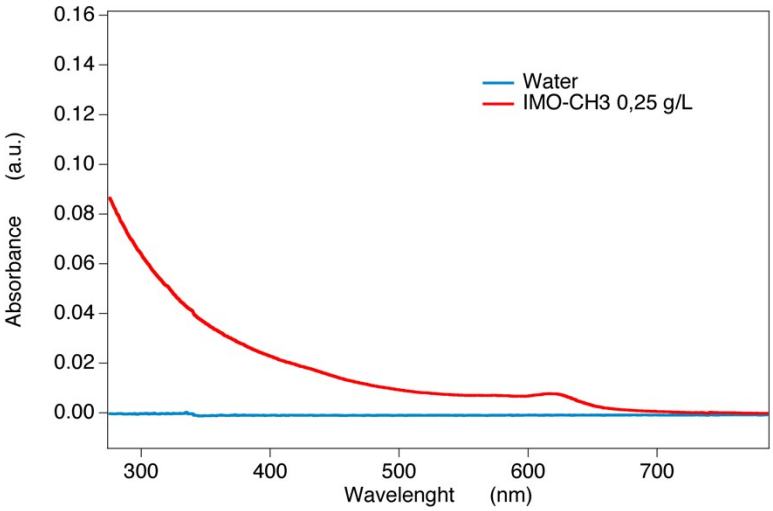

Figure S2 : Absorbance spectrum of pure water (blue) and a suspension of 0.25 g/L of imo_CH3 nanotube (red curve)

2°) Information about the length of the nanotube

In this work[2], an AFM study shows that the IMO-CH3 nanotube exhibits a characteristic length in the range of 200-300 nm. The Figure S2 is extracted from this work and the red line represented a 250 nm centered gaussian function.

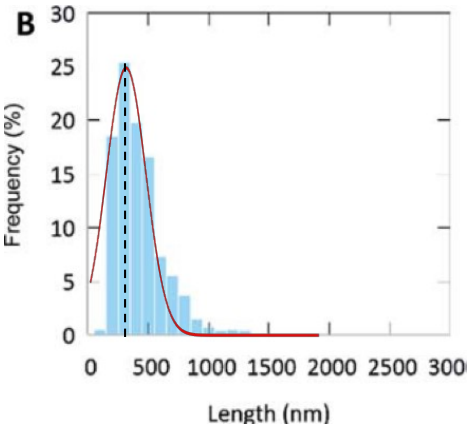

Figure S3 : IMO-CH3 distribution function determined by AFM

3°) Dependence of the polarization plots of Imo-CH3 suspension with different DO3 concentrations

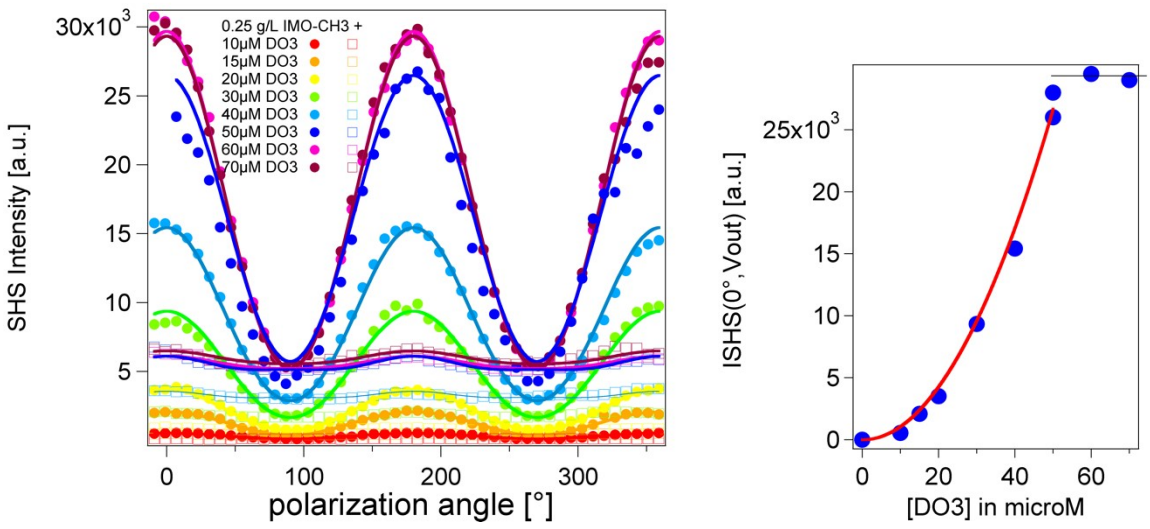

*Figure S4 Right: polarization plots for different DO3 concentrations in a 0.25 g/L Imo-CH3 suspension. Left: variation of I(0°,Vout) as a function of the DO3 concentration. The dots are the data. The red solid line is a quadratic fit function y=a*x*x. The black line is a eye guide to visualize the saturation of the signal.*

4°) Input parameter used for the PySHS package

The computation of the $I_{2,SHS}^{\Gamma}$ and $I_{4,SHS}^{\Gamma}$ coefficient are done with the PySHS V2.0 package freely available on Github[1]. The calculations are performed with the SHS module of the program, which considers an assembly of *N* fully correlated dipoles, each dipole representing a DO3 dye molecule. The input parameters are the hyperpolarizability of the DO3 molecule and the position and orientation of the *N* molecules. The other input parameters are the incident laser wavelength, here 800 nm, and the refractive index of the medium, taken here to be n=1.33.

5°) Procedure used to calculate the whole SHS Intensity from the PySHS software outputs

The PySHS software gives the SHS intensity for one supramolecular aggregate. The outputs of the software are the $a^{\Gamma},b^{\Gamma},c^{\Gamma}$ coefficients (where $\Gamma=V_{out}$ or H_{out}).

The SHS Intensity for one aggregate is thus given by :

[1] https://github.com/pmgassin/SHS_simulation.git

$$I_{SHS}(\alpha,\Gamma) = \left(a^{\Gamma}\, cos^4(\alpha) + b^{\Gamma}\, cos^2(\alpha)sin^2(\alpha) + c^{\Gamma}sin^4(\alpha)\right) \quad \text{(S1)}$$

For an assembly of N aggregates, the SHS intensity is given by

$$I_{SHS}(\alpha,\Gamma) = N\left(a^{\Gamma}\, cos^4(\alpha) + b^{\Gamma}\, cos^2(\alpha)sin^2(\alpha) + c^{\Gamma}sin^4(\alpha)\right) \quad \text{(S2)}$$

In all experiments presented in the manuscript, the total number of dye N_{dye} is fixed and equal to 0.05 mM. For an assembly of monodisperse aggregates, the total number of dye N_{dye} is linked to the number of aggregate N by:

$$N_{dye} = N \times N_{dye/agg} \quad \text{(S3)}$$

where $N_{dye/agg}$ is the number of dye in one aggregate.

For an assembly of N aggregates, the SHS intensity is given by

$$I_{SHS}(\alpha,\Gamma) = \frac{N_{dye}}{N_{dye/agg}}\left(a^{\Gamma}\, cos^4(\alpha) + b^{\Gamma}\, cos^2(\alpha)sin^2(\alpha) + c^{\Gamma}sin^4(\alpha)\right) \quad \text{(S4)}$$

6°) Additionnal computation done with PySHS package

The following simulation, table S1, shows that the ratio as defined in the manuscript don't have a significant effect on the $I^{\Gamma}_{2,SHS}$ and $I^{\Gamma}_{4,SHS}$ numerical values calculated. It has just an effect on the absolute SHS intensity without changing the shape of the polar plot.

Table S1 : the effect of the ratio, defined as the number of dipole "up" to the total number of dipole, onto the output $I_2^V, I_4^V, I_2^H, I_4^H$ coefficients.

	2D nanosheet model d=150 nm Ratio=0.52	2D nanosheet model d=150 nm Ratio=0.8	2D nanosheet model d=150 nm Ratio=1
I_2^V	0.48	0.47	0.47
I_4^V	-0.04	-0.04	-0.04
I_2^H	-0.29	-0.29	-0.29
I_4^H	0.01	0.01	0.01

a^v	880639	660463627	1853602077
b^v	1373637	1049016836	2933820173
c^v	292541	225081741	627716140
a^h	228962	174854351	489020748
b^h	628280	480204183	1337507446
c^h	416634	317053451	880334908

7°) Additional Molecular Dynamics simulation details

All MD simulations were carried out with GROMACS 2020.4 software. Atomistic simulations were initiated from a random configuration of solute in a box (with dimensions of 8 nm_ 8 nm _ 8 nm), solvated with water and ethanol molecule to meet the desired ethanol-water ratio mixture. Long-range electrostatic interactions were handled by the Particle Mesh Ewald (PME) method with a cut-off of 1.0 nm used for electrostatic and Lennard-Jones interactions. After minimization, a pre-equilibration run in the NVT ensemble was run using Nose–Hoover thermostat to keep the temperature constant at 300 K followed by a more extensive pre-equilibration in the NPT ensemble with the addition of the Parrinello–Rahman barostat to maintain a pressure of 1 bar. We used a leap-frog integrator with a time step of 1 fs for equilibration with an increase to 2 fs for production runs, where constraints were applied to all bonds using the Linear Constraints Solver (LINCS) algorithm. After equilibration, production simulations were typically performed for 20 ns. The simulation snapshot presented in Figure 2 is produced from the final frame of the MD trajectories.

References:

1. G. Martin-Gassin, E. Paineau, P. Launois and P.-M. Gassin, *The Journal of Physical Chemistry Letters*, 2022, **13**, 6883-6888.
2. P. Picot, O. Taché, F. Malloggi, T. Coradin and A. Thill, *Faraday Discussions*, 2016, **191**, 391-406.